Mechanism-Inspired Synthesis of Poly(alkyl malonates) via Alternating Copolymerization of Epoxides and Meldrum's Acid Derivatives

Sarah M. Severson[a], Bai-Hao Ren[a], May Cayzer[a], Ivan Keresztes[a], Mary L. Johnson[a], Xiao-Bing Lu[b], and Geoffrey W. Coates[a]*

[a]Department of Chemistry and Chemical Biology, Baker Laboratory, Cornell University, Ithaca, New York 14853-1301, United States

[b]State Key Laboratory of Fine Chemicals, Frontiers Science Center for Smart Materials, Dalian University of Technology, Dalian 116024, China

KEYWORDS: polymers, catalysis, ring-opening copolymerization, epoxides, Meldrum's acid

ABSTRACT: Direct incorporation of malonate units into polymer backbones is a synthetic challenge. Herein, we report the alternating and controlled anionic copolymerization of epoxides and Meldrum's acid (MA) derivatives to access poly(alkyl malonates) using (*N,N'*-bis(salicylidene)phenylenediamine)AlCl and a cyclopropenium chloride cocatalyst. This unique copolymerization yields a malonate-containing repeat unit while releasing a small molecule upon MA-derivative ring-opening. Mechanistic and computational studies reveal that the nature of the small molecule released influences overall polymerization kinetics, side reaction behavior, and molecular weight control. Controlled copolymerization of MA derivatives with a range of epoxides ultimately yields a library of new poly(alkyl malonates) with diverse and tunable thermal properties.

Introduction

The copolymerization of epoxides is a powerful approach to synthesize a diverse range of polymers.[1–3] In particular, extensive catalyst development has enabled exceptional activity and selectivity in the copolymerization of epoxides with anhydrides (Figure 1A) or carbon dioxide (CO_2) to yield polyesters and polycarbonates, respectively.[4–9] Chemists have since leveraged these catalytic approaches to copolymerize epoxides with other monomers such as carbonyl sulfide,[10–11] cyclic thioanhydrides,[12] lactones,[13–17] isothiocyanates,[18] and aldehydes[19] to synthesize new and/or underexplored polymers of interest.

Poly(alkyl malonates) are a class of polymers that remain inaccessible via controlled epoxide copolymerization. While these aliphatic polyesters show promise as polymer electrolytes in lithium-ion batteries and contain potentially degradable functionalities, their synthesis and exploration is challenging, as there are limited strategies to directly incorporate malonate units into polymer backbones.[20–24] As such, poly(alkyl malonates) are usually made via step-growth polymerization, a route that prohibits molecular weight control, precise architecture design, and facile substituent derivatization.[20, 25–27] Other approaches toward malonate-containing polymers—such as the polymerization of alkylidene malonates or malonate-substituted cyclopropanes—usually incorporate malonate units as side chains rather than into the main polymer backbone.[28–31] To the best of our knowledge, chain-growth approaches such as the ring-opening polymerization (ROP) of lactones and the ring-opening copolymerization (ROCOP) of epoxides and cyclic anhydrides have not yet been used to access poly(alkyl malonates), as many reported cyclic malonates are unstable under laboratory conditions.[32]

We envisioned that poly(alkyl malonates) could be accessed in a well-controlled fashion through the copolymerization of epoxides and Meldrum's acid (MA) derivatives, a class of malonate-containing heterocycles.[33–34] Owing to their facile derivatization, participation in multi-component reactions, and stimuli-triggered decomposition to aldehydes/ketones, CO_2, and/or ketenes, MA derivatives have been explored in polymer chemistry and engineering as monomers,[35–40] handles for post-polymerization reactivity,[41–46]

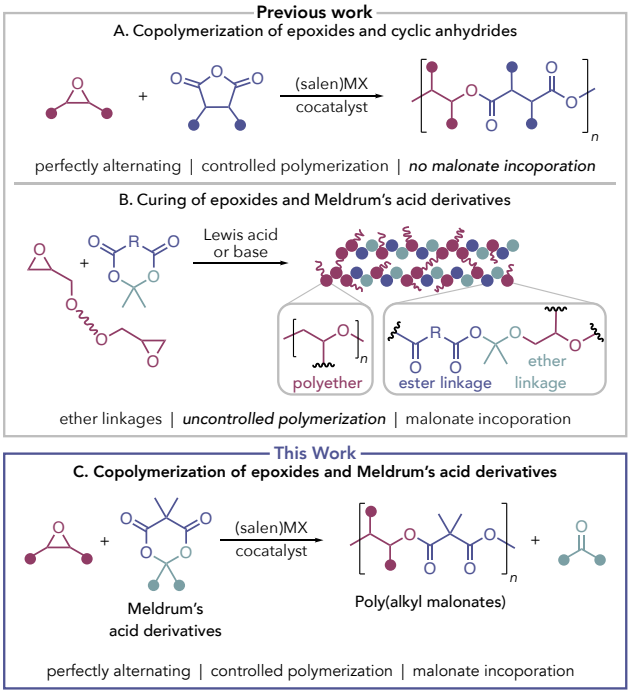

Figure 1. (a) Copolymerization of epoxides and anhydrides to access polyesters, (b) Curing of epoxides and MA derivatives to access poly(ether ester) resins, and (c) Copolymerization of epoxides and MA derivatives to access poly(alkyl malonates).

Table 1. Initial catalyst and CTA screen for PO/DMMA^{Me,Me} copolymerization.

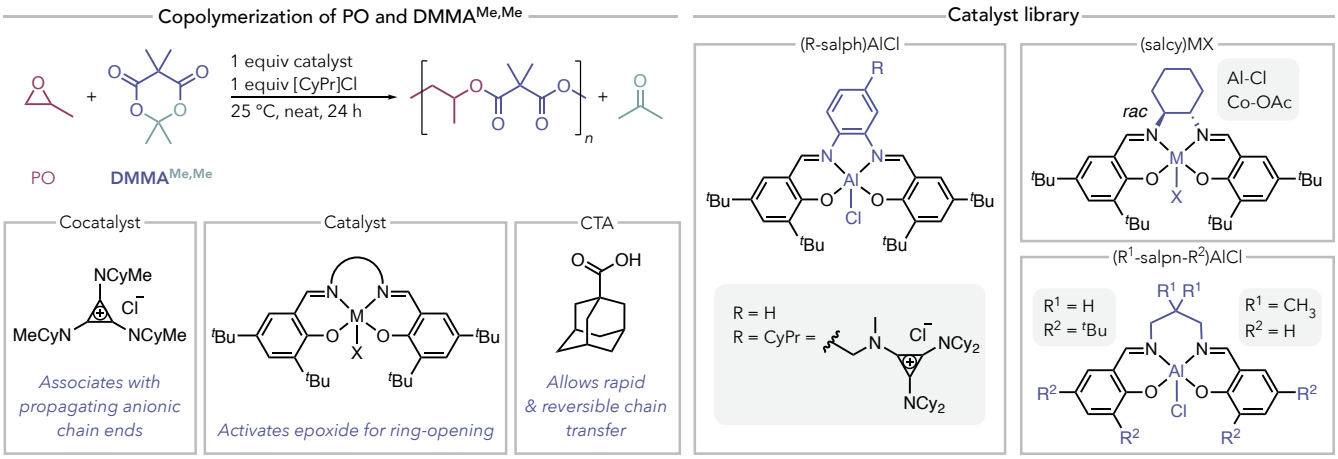

Entry[a]	Catalyst	Equiv DMMA^{Me,Me}	Equiv CTA	Conv of DMMA^{Me,Me} (%)[b]	$M_{n\,theo}$ (kDa)	$M_{n\,GPC}$ (kDa)[c]	$Đ$[c]
1	(H-salph)AlCl	100	0	28	2.4	2.7	1.13
2	(H-salph)AlCl	100	1	67	3.8	4.2	1.09
3	(H-salph)AlCl	100	10	86	1.2	1.9	1.18
4	(CyPr-salph)AlCl[d]	100	1	45	2.6	3.5	1.07
5	(salcy)CoOAc[e]	100	1	52	3.0	3.7	1.35
6	(salcy)AlCl	100	1	38	2.2	2.4	1.10
7	(H-salpn-^{t}Bu)AlCl	100	1	26	1.5	1.9	1.38
8	(CH_3-salpn-H)AlCl	100	1	12	0.7	1.4	1.21
9	(H-salph)AlCl	200	1	21	2.4	2.7	1.09

[a][PO]$_0$:[DMMA^{Me,Me}]$_0$:[catalyst]$_0$:[[CyPr]Cl]$_0$ = 5X:X:1:1 where X = equiv DMMA^{Me,Me}. [b]Determined by ^{1}H NMR spectroscopic analysis of crude polymerization mixtures. [c]Determined by GPC in THF, calibrated relative to monodisperse polystyrene standards. [d]No exogenous [CyPr]Cl added. [e]Trace epoxide homopolymerization observed.

and building blocks in thermoset design.[40,47–51] Hawker and coworkers demonstrated that MA derivatives can undergo decomposition to the corresponding ketene, which upon coupling with alcohols, yielded polyesters.[52–53] However, Serra and coworkers were the first to illustrate epoxide/MA derivative copolymerization during the Lewis acid- or base-initiated curing of diglycidyl ethers with MA derivatives, enabling access to malonate-containing crosslinked poly(ether ester) networks (Figure 1B).[50–51] When 4-dimethylaminopyridine (DMAP) was used as an initiator in these systems, it was postulated that acetone release could occur during ring-opening of MA derivatives.[54] Although this intriguing reactivity was not leveraged to access alternating poly(alkyl malonates), this example inspired us to explore MA derivatives as comonomers in controlled epoxide copolymerization.

We hypothesized that a controlled copolymerization of epoxides and MA derivatives to synthesize alternating poly(alkyl malonates) could be realized by using well-defined salenMX catalysts (salen = *N,N'*-bis(salicylidene)ethylenediamine) paired with nucleophilic cocatalysts. In epoxide/anhydride copolymerization, these catalyst/cocatalyst pairs initiate polymerization, activate the epoxide for ring-opening, and associate with propagating anionic chain ends (Figure 1A).[55] We predicted that these catalytic systems would function similarly in epoxide/MA derivative copolymerization. Based on precedent with anionic initators,[54] we also hypothesized that a (salen)MX catalyst paired with a nucleophilic cocatalyst could allow ring-opening of the MA derivative to proceed with ketone/aldehyde release to furnish the malonate moiety without the ether linkage, ultimately yielding alternating poly(alkyl malonates) (Figure 1C).

This strategy was further motivated by previous examples of small molecule elimination during ROP. For example, ROP of *O*-carboxyanhydrides is driven by loss of CO_2 and provides alternative access to poly(lactic acid).[56–57] Hillmyer and coworkers similarly illustrated that ROP of a cyclic esteracetal occurs with loss of acetaldehyde at high catalyst loadings.[58] During the ring-opening polymerization of 1,3-dioxolan-4-ones, Shaver and coworkers leveraged small molecule release to access a range aliphatic and alicyclic polyesters.[59–63]

Herein, we report a chain-growth approach in which epoxides are copolymerized with MA derivatives to yield highly alternating poly(alkyl malonates) while releasing a small molecule (Figure 1C). Kinetic and computational mechanistic studies reveal that the identity of the small molecule released during copolymerization significantly impacts polymerization behavior. We propose a mechanism for this transformation which is distinct from what is known for epoxide/anhydride copolymerization. Evaluation of a series of epoxide comonomers yielded a diverse library of poly(alkyl malonates) with tunable thermal properties, highlighting the utility of epoxide/MA derivative ROCOP.

Results and Discussion

Initial Copolymerization Optimization. Initial copolymerization screenings were performed with propylene oxide (PO) and 2,2,5,5-tetramethyl-1,3-dioxane-4,6-dione, otherwise termed dimethyl Meldrum's acid (DMMA^{Me,Me}) (Table 1). DMMA^{Me,Me} was selected to avoid unwanted reactivity with acidic protons of unmethylated MA and was readily synthesized on a multi-gram scale from commercially-available MA (see Supporting Information).[64] In

epoxide/anhydride ROCOP, anhydride ring-opening by an alkoxide intermediate produces a carboxylate species that performs rate-determining epoxide ring-opening.[55] We hypothesized that DMMA^{R,R} (where ^{R,R} notates the substituents of the ketone/aldehyde releasing during the polymerization) ring-opening followed by ketone/aldehyde release would produce a carboxylate intermediate that would preferentially perform epoxide ring-opening (*vide infra*). Thus, a range of (salen)MX catalysts with cyclopropenium chloride ([CyPr]Cl) as a cocatalyst were screened at 25 °C (Table 1). [CyPr]Cl was selected as a cocatalyst due to its demonstrated suppression of transesterification during epoxide/anhydride copolymerization as compared to other common cocatalysts.[65] This same transesterification suppression is observed in PO/DMMA^{R,R} copolymerization at elevated temperatures, rationalizing the selection of [CyPr]Cl (*vide infra*).

However, most catalyst/cocatalyst pairs studied exhibited poor activity for PO/DMMA^{Me,Me} ROCOP, even at high catalyst loadings (Table 1, entry 1, and Table S1, entries 4, 7, and 10). Inspired by a report from Darensbourg and coworkers in which exogenous chain transfer agents (CTAs) were required to initiate epoxide/CO_2 copolymerization, one equivalent of adamantane carboxylic acid ($AdCO_2H$) was added as a CTA to PO/DMMA^{Me,Me} copolymerizations.[66] Conversion to polymer improved with most catalysts studied (Table 1, entry 2, Table S1, entries 1–12, and Table SX, entries 1–2). As acceleration by CTA is not generally observed in copolymerization of PO, we rationalized that this reactivity was connected to DMMA^{Me,Me} ring-opening and subsequent acetone release. Because (salen)AlX catalysts paired with nucleophilic cocatalysts usually propagate as anionic, 6-coordinate species,[55] it is likely that DMMA^{Me,Me} ring-opening first yields a 6-coordinate alkoxide intermediate that may not readily facilitate acetone release if an open coordination site is unavailable to accept the resulting carboxylate (Scheme S2). As such, we hypothesize that CTAs may provide a proton to facilitate acetone release, accelerating turnover of the catalytic cycle (Scheme S2). Further, we also hypothesize that the CTA may function to protonate strongly coordinating species that inhibit epoxide binding to the catalyst (*vide infra*) Consistent with detailed studies of CTA function in epoxide/anhydride ROCOP, minimal differences in polymerization activity were observed when a carboxylic acid ($AdCO_2H$) versus an alcohol (1,6-hexanediol (1,6-HD)) was used, as each CTA ultimately reacts to yield the same dormant chain ends (Table S1, entry 15, and Scheme S1).[67–68] As excess CTA offered a negligible increase in activity at 25 °C and decreased polymer molecular weight (Table 1, entry 3), one equivalent of CTA was chosen for standard conditions.

Subsequent catalyst screening with one equivalent of $AdCO_2H$ revealed the initial selection of (salph)AlCl with [CyPr]Cl enables fastest conversion to polymer and good molecular weight control (Table 1, entry 2). Bifunctional (CyPr-salph)AlCl demonstrates slower polymerization than its binary analogue (Table 1, entry 4).[65] Likewise, Co- and Al- catalysts featuring nonplanar ONNO geometries (such as salcy or salpn ligands) exhibit slower polymerization than (salph)AlCl; these results are consistent with previous studies which indicate that distorted ONNO orientations can slow epoxide activation (Table 1, entries 5–8).[65,69] While catalysts featuring salpn backbones have shown good activity in copolymerization of 3-dioxolan-4-ones with lactones,[62–63] their slower activity in PO/DMMA^{Me,Me} copolymerization emphasizes a need to balance both acceleration of epoxide-binding and facilitation of small-molecule release (Table 1, entries 7–8). As (salph)AlCl/[CyPr]Cl demonstrated the highest conversion to polymer in 24 hours and yielded an extremely narrow dispersity ($Đ$ = 1.09), this catalyst/cocatalyst pair with one equivalent of CTA was selected for all following polymerizations (Table 1, entry 2).

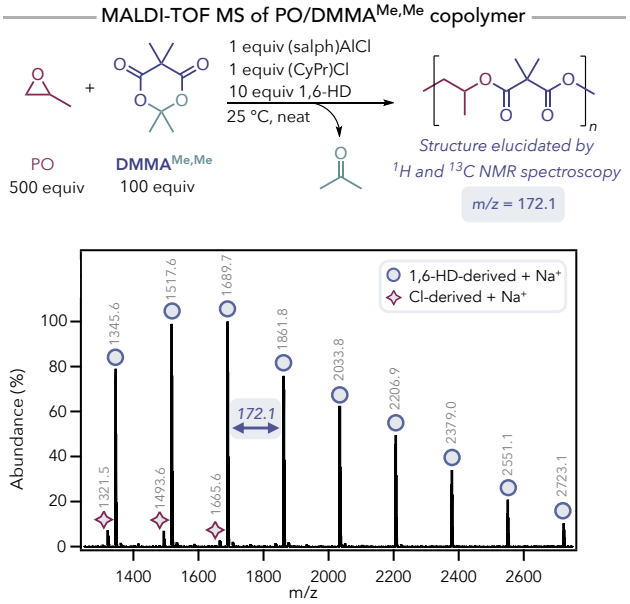

Figure 2. MALDI-TOF mass spectrum of PO/DMMA^{Me,Me} copolymer.

Kinetic Behavior of PO/DMMA^{Me,Me} Copolymerization. We sought to validate the proposed repeat unit in which acetone is released rather than incorporated into the main polymer chain. ^{1}H NMR spectroscopic analysis of crude polymerization mixtures showed the formation of acetone alongside the expected polymer repeat unit (Figure S32). ^{1}H and ^{13}C{^{1}H} NMR spectroscopy of precipitated PO/DMMA^{Me,Me} copolymers corroborate the copolymer repeat unit in which acetone is released rather than incorporated (Figures S34-35). MALDI-TOF MS analysis of low-molecular weight PO/DMMA^{Me,Me} copolymers prepared with 10 equivalents of 1,6-hexanediol (1,6-HD) as CTA is consistent with this proposed PO/DMMA^{Me,Me} repeat unit (m/z = 172.1) (Figure 2, Figure S29). Although it is possible that MALDI-TOF MS is unable to detect any incorporated acetone linkages, the combination of ^{1}H and ^{13}C{^{1}H} NMR spectroscopy and MALDI-TOF MS provides strong evidence for the proposed repeat unit. MALDI-TOF analysis confirms the presence of both CTA and Cl^- (from catalyst and cocatalyst) initiated chains. As the copolymerization is performed in an excess of epoxide to full conversion, PO-derived hydroxyl end groups are observed for both Cl^- and CTA-initiated chains.

Even with the occurrence of small molecule release, PO/DMMA^{Me,Me} copolymerization with (salph)AlCl and [CyPr]Cl is well-controlled. At 25 °C, conversion (%) of DMMA^{Me,Me} to polymer increases linearly with time (Figure 3A) and molecular weight increases linearly with conversion (Figure 3B). The resulting polymer boasts a narrow and unimodal molecular weight distribution ($Đ$ = 1.09) (Figure 3C and Table S2). These results are consistent with controlled polymerization in which each equivalent of initiator (Cl^- from catalyst/cocatalyst and CTA) produces one active chain. Sequential DMMA^{Me,Me} addition results in full monomer consumption ion, further corroborating active chain ends (Figure S3).

The observed linear conversion versus time (Figure 3A) is consistent with pseudo-zero order kinetics, as expected in epoxide copolymerization when epoxide is in excess. For example, while epoxide/anhydride copolymerization with (salph)AlCl and bis(triphenylphosphine)iminium chloride ([PPN]Cl) as a cocatalyst exhibits a first-order dependence on epoxide and a zero-order dependence on anhydride, the use of excess epoxide results in overall

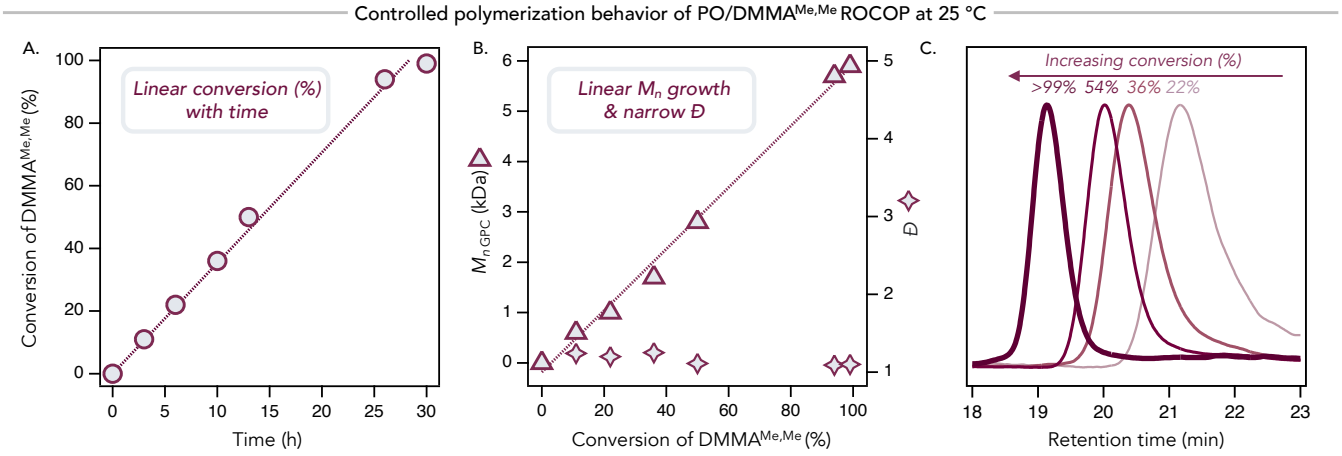

Figure 3. $[PO]_0:[DMMA^{Me,Me}]_0:[(salph)AlCl]_0:[[CyPr]Cl]_0:[AdCO_2H]_0$ = 500:100:1:1:1 and T = 25 °C for (a) Conversion of DMMA^{Me,Me} versus time (b) $M_{n\,GPC}$ (kDa) versus conversion of DMMA^{Me,Me} (c) GPC chromatograms with increasing monomer conversion, calibrated relative to monodisperse polystyrene standards.

pseudo zero-order polymerization kinetics.[55] Preliminary rate-law determination experiments performed with one equivalent of CTA confirm a first-order dependence on PO and a zero-order dependence on DMMA^{Me,Me} (Figure S5). These kinetic results indicate that in PO/DMMA^{Me,Me} ROCOP catalyzed by (salph)AlCl/[CyPr]Cl with 1 equivalent of $AdCO_2H$, epoxide binding and ring-opening is likely rate-determining.

However, PO/DMMA^{Me,Me} copolymerization at 25 °C is slow, thus preventing the targeting of higher molecular weights in reasonable timeframes (Table 1, entry 9, Table S4, entries 1–2). When PO/DMMA^{Me,Me} copolymerizations were performed at 60 °C to accelerate polymerization, we were surprised to find that conversion to polymer no longer exhibited a linear relationship with time and required nearly 30 hours to consume 100 equivalents of DMMA^{Me,Me} (Figure 4A, 1 equivalent CTA). These results indicate that raising the polymerization temperature from 25 °C to 60 °C caused a deviation from the previously observed pseudo zero-order polymerization kinetics.

Further investigation revealed that this unexpected deviation from zero order kinetics was accompanied by a decarboxylation side reaction. GPC chromatograms of PO/DMMA^{Me,Me} copolymers made at 60 °C exhibit low-molecular weight tailing that is not observed at 25 °C (Figure S8). Furthermore, ^{1}H NMR spectroscopy of crude polymerization mixtures ran at 60 °C reveal the formation of trace propylene carbonate, a byproduct of PO/CO_2 coupling (Figure S9).[70] Given the documented decarboxylation of MA derivatives, these results suggest that carboxylate intermediates can undergo decarboxylation (Figure 4B, Pathway B) rather than perform epoxide ring-opening (Figure 4B, Pathway A).[71-72] Decarboxylation would presumably form CO_2 and an Al enolate that likely cannot continue polymerization; instead, protonation by CTA is required to remove the inactive chain from the metal center, resulting in polymer chain termination (Figure 4B).

In support of this hypothesis, MALDI-TOF MS of PO/DMMA^{Me,Me} copolymers made at 60 °C contain a low-intensity series consistent with decarboxylated, terminated PO/DMMA^{Me,Me} copolymers (Figure S30); this series is not detected in mass spectra of copolymers made at 25 °C (Figures S29). Furthermore, the expected isopropyl end groups were also visible by ^{1}H NMR spectroscopy of precipitated PO/DMMA^{Me,Me} copolymers made at 60 °C (Figure S10). To further support this hypothesis, PO/DMMA^{Me,Me} copolymerization was run at 100 °C with 10 equivalents of CTA to increase the concentration of terminated, decarboxylated end groups. 2D NMR spectroscopy of the resulting isolated PO/DMMA^{Me,Me} copolymers further corroborated the structure of isopropyl ester end groups that form by decarboxylation and subsequent protonation (Table S18, and Figures S40-S44). These results indicate that while protonation liberates the catalyst to continue propagation, it does so at the cost of termination of another polymer chain.

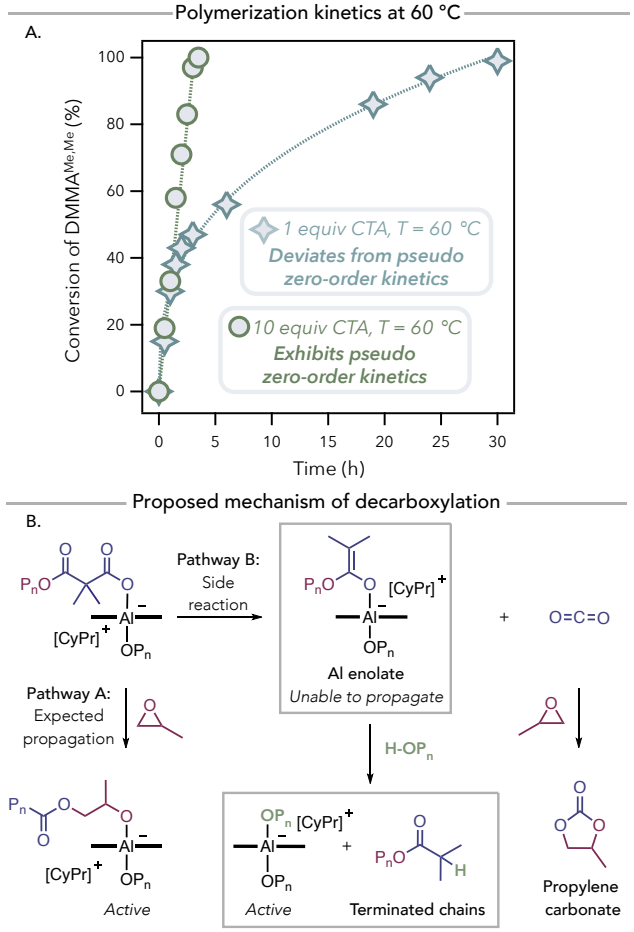

Figure 4. (a) Restoration of pseudo zero-order kinetics when $[PO]_0:[DMMA^{Me,Me}]_0:[(salph)AlCl]_0:[[CyPr]Cl]_0:[AdCO_2H]_0$ = 500:100:1:1:10 and T = 60 °C and (b) Proposed mechanism of decarboxylation.

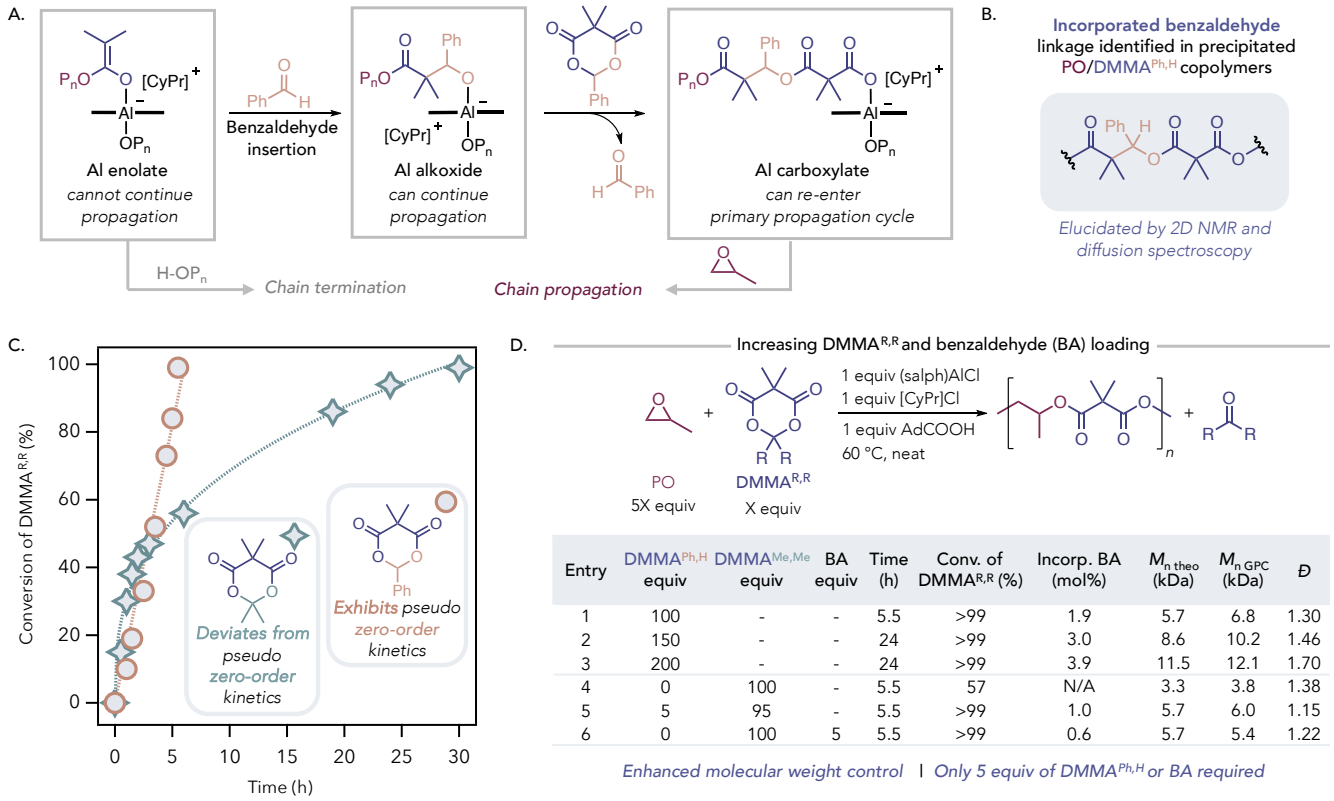

Entry	DMMA^{Ph,H} equiv	DMMA^{Me,Me} equiv	BA equiv	Time (h)	Conv. of DMMA^{R,R} (%)	Incorp. BA (mol%)	$M_{n\ theo}$ (kDa)	$M_{n\ GPC}$ (kDa)	$Đ$
1	100	-	-	5.5	>99	1.9	5.7	6.8	1.30
2	150	-	-	24	>99	3.0	8.6	10.2	1.46
3	200	-	-	24	>99	3.9	11.5	12.1	1.70
4	0	100	-	5.5	57	N/A	3.3	3.8	1.38
5	5	95	-	5.5	>99	1.0	5.7	6.0	1.15
6	0	100	5	5.5	>99	0.6	5.7	5.4	1.22

Enhanced molecular weight control | *Only 5 equiv of DMMA^{Ph,H} or BA required*

Figure 5. (a) Chain termination suppressed by benzaldehyde insertion, (b) Inserted benzaldehyde linkage elucidated by 2D NMR spectroscopy, (c) Conversion (%) of DMMA^{R,R} versus time when $[PO]_0$:$[DMMA^{R,R}]_0$:$[(salph)AlCl]_0$:$[[CyPr]Cl]_0$:$[AdCO_2H]_0$ = 500:100:1:1:1 and T = 60 °C (d) M_n control and incorporation (incorp.) of benzaldehyde (BA) (mol%) with varying amounts of DMMA^{R,R} and BA.

Although malonate decarboxylation at 60 °C occurs only to a small portion of chain ends, we anticipate that it influences polymerization kinetics such that zero-order kinetics are suppressed. First, the resulting enolate may coordinate to the catalyst, preventing epoxide binding until protonation occurs; second, protonation to produce a terminated chain reduces the overall concentration of CTA, an important additive for polymerization. To confirm this hypothesis, copolymerizations were performed with 10 equivalents of CTA at 60 °C, where changes to CTA concentration are negligible and decarboxylated intermediates can more readily be protonated. Excitingly, this copolymerization exhibits pseudo zero-order kinetic behavior (Figure 4A, 10 equivalents of CTA). Although CTAs may influence the polymerization through other chain-transfer events, this result suggests that mediation of the decarboxylation side reaction is important for maintaining zero-order polymerization kinetics. Unfortunately, use of excess CTA produces low molecular-weight polymers with increased chain termination, rendering this approach to mediating decarboxylation impractical.

Design and Polymerization of Benzaldehyde-releasing DMMA^{Ph,H}. To restore zero-order kinetic behavior while maintaining molecular weight control, we sought out synthetic strategies to allow the Al enolate to continue propagation with suppressed chain termination. As (salen)Al enolates readily react with aldehydes, we aimed to modify DMMA^{R,R} such that a reactive aldehyde is released during polymerization.[73] Therefore, PO was copolymerized with 5,5-dimethyl-2-phenyl-1,3-dioxane-4,6-dione (DMMA^{Ph,H}), a MA derivative that releases benzaldehyde instead of acetone upon ring-opening but yields the same repeat unit accessed by PO/DMMA^{Me,Me} copolymerization. We hypothesized that benzaldehyde insertion after decarboxylation would produce an Al alkoxide that can continue propagation, thereby restoring pseudo zero-order kinetic behavior (Figure 5A).

Copolymerization of PO and DMMA^{Ph,H} at 60 °C with one equivalent of CTA yielded the expected copolymer alongside benzaldehyde formation (Figure S33). ^{1}H and ^{13}C{^{1}H} NMR spectroscopy of precipitated PO/DMMA^{Ph,H} copolymers corroborate the copolymer repeat unit consistent with benzaldehyde release (Figures S45-46). Furthermore, MALDI-TOF MS analysis of low-molecular weight PO/DMMA^{Ph,H} copolymer is consistent with the proposed repeat unit (m/z = 172.1) (Figure S31). The low-intensity series corresponding to decarboxylated, terminated chains previously observed at 60 °C with the PO/DMMA$^{Me,\ Me}$ copolymer is no longer observed in the MALDI-TOF MS of the PO/DMMA^{Ph,H} polymer, suggesting suppressed chain termination.

Indeed, ^{1}H NMR spectroscopy of precipitated PO/DMMA^{Ph,H} copolymers revealed trace incorporation of aromatic protons (presumably from benzaldehyde insertion) within the polymer (Figure S45). Extensive 2D NMR spectroscopic analysis confirmed that the observed benzaldehyde incorporation is consistent with decarboxylation, subsequent benzaldehyde insertion, and further propagation with another DMMA^{R,R} (Figure 5B, Figures S49–S64, Scheme S3). Additionally, ^{1}H NMR diffusion spectroscopy revealed that this observed linkage exhibits a diffusion coefficient very similar to that of the primary epoxide/DMMA^{R,R} protons in the main polymer backbone (Figure S65–S67). This analytical evidence supports our hypothesis that benzaldehyde insertion into decarboxylated intermediates allows propagation to continue with reduced chain termination, enabling re-entry into the primary propagation cycle (Scheme 1).

Excitingly, this continued propagation after benzaldehyde insertion was indeed accompanied by pseudo zero-order polymerization kinetics. During PO/DMMA^{Ph,H} copolymerization at 60 °C, conversion (%) to polymer increased linearly with time and molecular

Scheme 1. Simplified Proposed Mechanism of Epoxide and DMMA^{R,R} Copolymerization (where CTA is neglected and PO and DMMA^{Me,Me} Are Used for Simplicity), Including the Primary Propagation Cycle and Return to the Primary Propagation Cycle via Benzaldehyde Insertion into Decarboxylated Catalytic Intermediates.

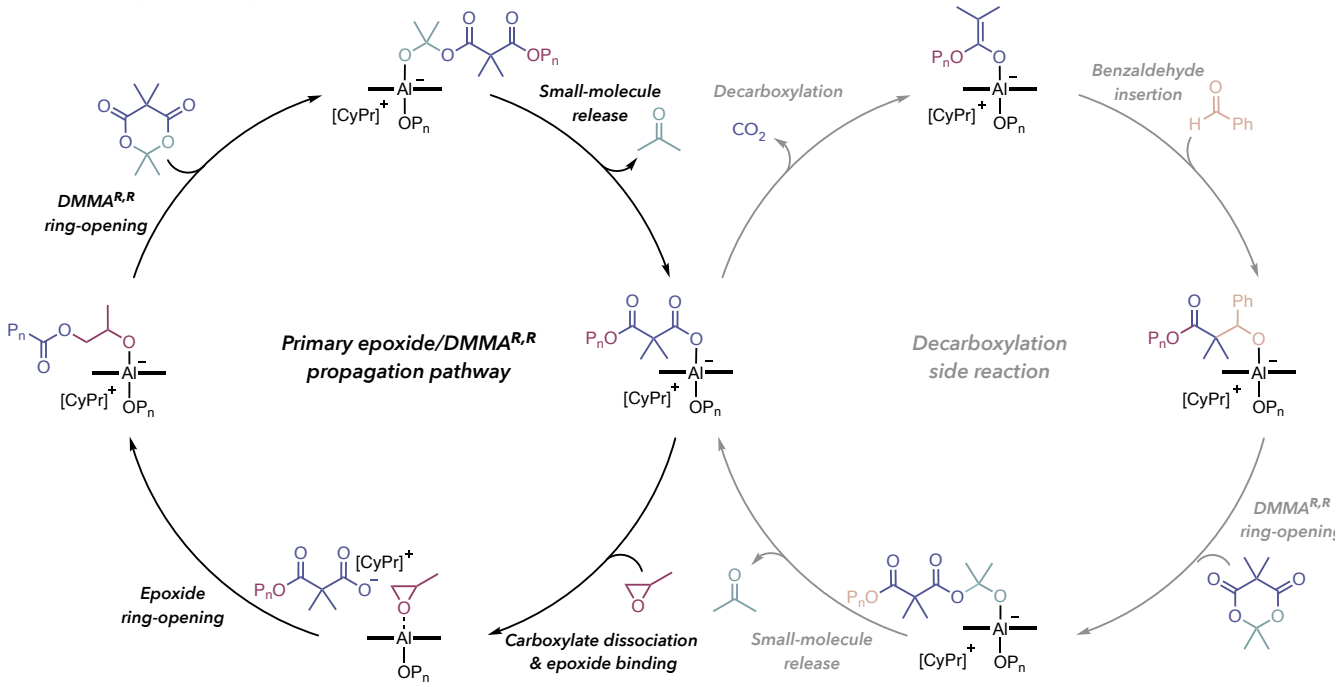

weight increased linearly with conversion (Figure 5C, Figure S12). The observed pseudo zero-order kinetic behavior of PO/DMMA^{Ph,H} copolymerization enabled an enhanced rate of polymerization: only 5.5 h was required to consume 100 equivalents of DMMA^{Ph,H}, whereas 30 h was required for PO/DMMA^{Me,Me} copolymerization under the same conditions (T = 60 °C, 1 equivalent CTA) (Figure 5C). PO/DMMA^{Ph,H} copolymerization still required 1 equivalent of CTA for productive polymerization, confirming that CTA participates in other chain-transfer events (besides protonation of decarboxylated intermediates) that are needed for polymerization (Table S11, entries 1–2).

With this improved kinetic behavior, molecular weights above 10 kDa were targeted within 24 h, a feat unattainable with the previous acetone-releasing DMMA^{Me,Me} (Figure 5D, entries 1–3, and Figure S14 versus Figure S4). Interestingly, the extent of benzaldehyde incorporated into the polymer increased as monomer loading increased, suggesting that decarboxylation may increase alongside monomer loading (Figure 5D, entries 1–3). GPC traces of PO/DMMA^{Ph,H} copolymers are bimodal, due to either trace protic impurities that lead to bimolecular polymer growth and/or chain-end coupling occurring as full conversion is reached (Figures S12 and S16).[8,65] Despite rigorous monomer purification, bimodality in GPC traces is standard in most epoxide copolymerizations and well-documented in the literature. [68] Despite this bimodality, use of [CyPr]Cl compared to other common cocatalysts allowed the narrowest molecular weight distribution; dispersity broadening consistent with increased transesterification is observed when [PPN]X cocatalysts are used (Table S9, entries 5–9 and Figure S13).

As decarboxylation occurs only minimally during polymerization, we anticipated that DMMA^{Ph,H} does not need to be utilized in excess during polymerization. Indeed, copolymerization of 95 equivalents of DMMA^{Me,Me} with just 5 equivalents of DMMA^{Ph,H} reached full conversion in the same amount of time as polymerization of 100 equivalents of DMMA^{Ph,H} and afforded an improved polymer dispersity (Figure 5D, entry 4 versus entry 1, and Figure S17). Directly adding 5 equivalents of benzaldehyde to 100 equivalents of DMMA^{Me,Me} produced similar results, albeit with slightly reduced benzaldehyde incorporation, validating the role of benzaldehyde as an enolate scavenger (Figure 5D, entry 6). As the ratio of 95:5 DMMA^{Me,Me}:DMMA^{Ph,H} afforded the narrowest molecular weight distribution of all conditions studied, this was selected as the standard loading for future polymerizations. Increasing monomer loading from 100 to 200 equivalents while maintaining this 5:95 DMMA^{Ph,H}:DMMA^{Me,Me} ratio increased polymer molecular weight (Table S14, entries 1–3).

DFT Calculations of Epoxide Ring-Opening. In efforts to further understand the effect of benzaldehyde insertion on polymerization kinetics, we turned to DFT calculations to elucidate how proposed catalytic intermediates might influence epoxide ring-opening. Previous mechanastic studies suggest the epoxide likely binds to the (salph)Al catalyst *trans* relative to another chain end (represented as X in Figure 6) coordinated to the same Al center. Furthermore, extensive mechanistic and computational studies of epoxide/anhydride copolymerization revealed that the *trans* anion X can possibly raise or lower the barrier to epoxide binding and ring-opening by attenuating the Lewis acidity of the Al center.[55] DFT analysis (see Supporting Information for computational details) was therefore used to examine the barriers of epoxide ring-opening while varying the identity of *trans* anion X derived from relevant PO/DMMA^{R,R} catalytic intermediates (Figure 6). Anions investigated included those derived from PO ring-opening (X1), DMMA^{R,R} ring-opening (X2–X4), and DMMA^{R,R} decarboxylation (X5–X8). We predicted that the formation of an alkoxide intermediate may occur prior to small-molecule release, and these proposed intermediates were included in DFT analysis (Scheme 1). A detailed computational analysis of the full mechanistic cycle is currently in progress.

The alkoxide (X1) and carboxylate (X2) intermediates derived from PO and DMMA^{R,R} ring-opening show high energy barriers of 35.8 and 34.2 kcal/mol, respectively (Figure 6). These energy barriers are higher than conventional alkoxide and carboxylate intermediates in epoxide/anhydride copolymerization, presumably due to the increased steric bulk of DMMA^{R,R}.[55] These higher energy

Table 2. Epoxide/ DMMA^{R,R} copolymerization scope.

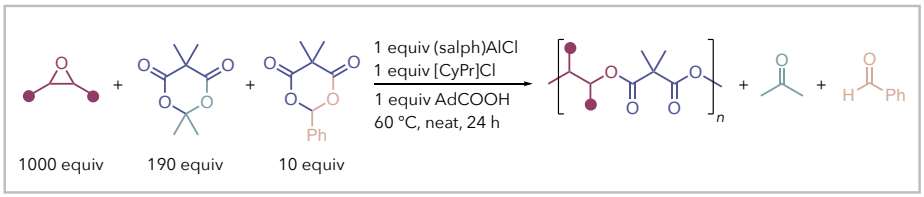

Entry	Epoxide	Conv of DMMA^{R,R} (%)[a]	$M_{n\,theo}$ (kDa)	$M_{n\,GPC}$ (kDa)[b]	$Đ$[b]	T_g (°C)[c,d]	T_m (°C)[c,e]
1	*rac*-PO	>99	11.5	7.9	1.39	−4.9	-
2	*rac*-BO	94	11.7	6.7	1.38	−13.6	-
3	*rac*-AGE	>99	15.2	5.9	1.41	−32.9	-
4	*rac*-PGE	>99	17.6	8.8	1.50	19.8	-
5	*(R)*-PO	>99	11.5	7.3	1.35	−4.6	98.2 / 86.2
6	*(S)*-PO	>99	11.5	7.2	1.31	−4.3	98.9 / 86.9
7	*cis*-BO[f]	52	6.5	3.8	1.47	9.5	97.4

[a]Determined by ^{1}H NMR spectroscopic analysis. [b]Determined by GPC in THF, calibrated relative to monodisperse polystyrene standards. [c]Polymers isolated and thoroughly dried prior to DSC analysis. [d]Determined by DSC. [e]Determined by DSC, major polymorph / minor polymorph. [f]Polymerization time = 48 h.

barriers are consistent with PO/DMMA^{R,R} ROCOP's slower catalytic activity compared to that of PO/anhydride ROCOP with the same catalyst system.[65] Additionally, the alkoxide intermediate (X3) arising from DMMA^{Ph,H} ring-opening also shows a high energy barrier of 33.3 kcal/mol, whereas the semi-acetal anion (X4, from DMMA^{Me,Me} ring-opening) shows a relatively lower energy barrier (29.9 kcal/mol).

Interestingly, lower barriers to ring-opening were generally achieved with intermediates derived from decarboxylation (X5–X7). In particular, the lowest energy barrier is obtained by X7, the intermediate obtained from decarboxylation and subsequent benzaldehyde insertion, suggesting that X7 coordination to the Al center possibly leads to a rate enhancement (Figure 6). By contrast, X8 exhibits a higher energy barrier, providing potential rationale for the lack of acetone insertion observed during PO/DMMA^{Me,Me} ROCOP. The accelerated polymerization rate observed when benzaldehyde is added exogenously to PO/DMMA^{Me,Me} copolymerization at 60 °C lends further support to X7's possible role as an accelerant of epoxide ring-opening (*vide supra*). Taken together, these computational insights suggest that benzaldehyde insertion and decarboxylation not only enable propagation to continue, but possibly yields catalyst-coordinated chain-ends that can accelerate epoxide ring-opening.

Copolymerization Scope and Polymer Properties. With an optimized copolymerization system in hand, various epoxides were copolymerized at a loading of 10:190 DMMA^{Ph,H}:DMMA^{Me,Me} to access a library of new poly(alkyl malonates). Copolymerization with *rac*-PO or *rac*-butene oxide (*rac*-BO) yielded copolymers with glass transition temperature (T_g) values of −4.9 and −13.6 °C, respectively (Table 2, entries 1–2, Figure S20 and Figure S21). Copolymerization with *rac*-allyl glycidyl ether (*rac*-AGE)—whose incorporation provides handles for post-polymerization modification—yielded a copolymer with an even lower T_g value of −32.9 °C (Table 2, entry 3 and Figure S22). Materials with T_g values below room temperature are desirable, as these materials can be used as a midblock in thermoplastic elastomers; furthermore, low T_g values are generally associated with improved segmental relaxation and therefore increased lithium conductivity for battery applications.[3,74] Copolymerization with *rac*-phenyl glycidyl ether (*rac*-PGE) resulted in a material with an increased T_g of 19.8 °C relative to aliphatic copolymers, presumably due to increased steric bulk reducing segmental motion (Table 2, entry 4 and Figure S23).

Epoxide/DMMA^{R,R} copolymerization can also be used to access semicrystalline polyesters. Copolymerization with (*R*)- or (*S*)-PO yielded copolymers with melting temperatures (T_m's) of approximately 98 °C (Table 2, entries 5–6, Figure S24 and Figure S25). This system is also compatible with disubstituted epoxides, although conversion to polymer is slowed relative to terminal epoxides (Table 2, entry 7). Copolymerization with *cis*-buteneoxide (*cis*-BO) yielded a polymer with relatively low M_n (3.8 kDa) but exhibited an unexpectedly high T_m of 97.4 °C (Table 2, entry 7 and Figure S26). Ring-

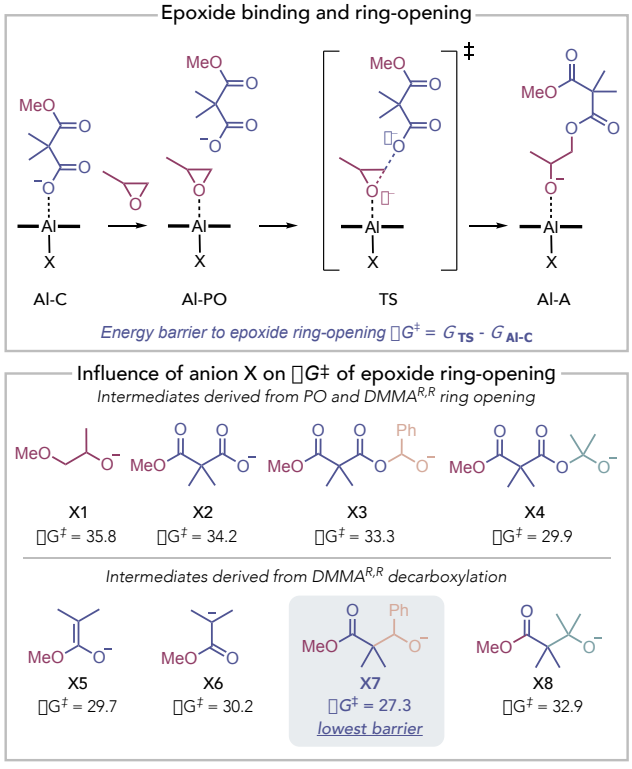

Figure 6. DFT calculations of rate-determining step of PO/DMMA^{R,R} copolymerization with different anions, X1–X8; Gibbs free energy values given in kcal/mol.

opening of a *meso* epoxide with an achiral catalyst is predicted to occur with net inversion, yielding a copolymer with a *racemic* mixture of *trans*-2,3 dimethyl units. Although this material was expected to be amorphous based on the results with *rac*-PO, tacticity-independent crystallinity has recently been reported for PHAs.[75–76] Taken together, the copolymerization of epoxides with $DMMA^{R,R}$ is a viable route to access new poly(alkyl malonates) with tunable thermal properties.

Conclusions

We have developed a new method to copolymerize epoxides with MA derivatives to produce alternating poly(alkyl malonates). The kinetic behavior of epoxide/$DMMA^{R,R}$ ROCOP is influenced by the identity of the small molecule released: at 60 °C, PO copolymerization with acetone-releasing $DMMA^{Me,Me}$ deviates from the expected zero-order polymerization kinetics, whereas PO copolymerization with benzaldehyde-releasing $DMMA^{Ph,H}$ exhibits zero-order behavior. This phenomenon is attributed to the insertion of benzaldehyde into decarboxylated catalytic intermediates, which allows re-entry into the primary propagation cycle. Furthermore, DFT calculations suggest that the catalytic intermediate resulting from $DMMA^{R,R}$ decarboxylation and subsequent benzaldehyde insertion may accelerate rate-determining epoxide ring-opening. Epoxide/$DMMA^{R,R}$ copolymerization was ultimately used to assemble a polymer library of new poly(alkyl malonates), where varying the epoxide substituent(s) allowed tuning of thermal properties. Ongoing work focuses on full mechanism elucidation, exploring new catalytic systems for improved activity and molecular weight targeting, and expanding monomer scope to access new copolymers and stereocomplexes with competitive properties. We envision that these findings will allow further understanding of epoxide/$DMMA^{R,R}$ copolymerization and streamline access to poly(alkyl malonates).

ASSOCIATED CONTENT

Supporting Information

The Supporting Information is available free of charge on the ACS Publications website. Experimental procedures; polymer characterization; spectral data; and other supporting data (PDF)

AUTHOR INFORMATION

Corresponding Author

Geoffrey W. Coates – *Department of Chemistry and Chemical Biology, Baker Laboratory, Cornell University, Ithaca, New York 14853 – 1301, United States;* orcid.org/0000-0002-3400-2552; Email: coates@cornell.edu

Authors

Sarah M. Severson – *Department of Chemistry and Chemical Biology, Baker Laboratory, Cornell University, Ithaca, New York 14853 – 1301, United States; orcid.org/0000-0001-9305-6270*

Bai-Hao Ren – *Department of Chemistry and Chemical Biology, Baker Laboratory, Cornell University, Ithaca, New York 14853 – 1301, United States, https://orcid.org/0009-0001-9301-6276*

May Cayzer – *Department of Chemistry and Chemical Biology, Baker Laboratory, Cornell University, Ithaca, New York 14853 – 1301, United States, https://orcid.org/0009-0009-7001-9034*

Ivan Keresztes – *Department of Chemistry and Chemical Biology, Baker Laboratory, Cornell University, Ithaca, New York 14853 – 1301, United States, https://*orcid.org/*0000-0002-1271-3847*

Mary L. Johnson – *Department of Chemistry and Chemical Biology, Baker Laboratory, Cornell University, Ithaca, New York 14853 – 1301, United States, https://orcid.org/0000-0003-0939-2605*

Xiao-Bing Lu – *State Key Laboratory of Fine Chemicals, Frontiers Science Center for Smart Materials, Dalian University of Technology, Dalian 116024, China https://orcid.org/0000-0001-7030-6724*

Notes

The authors declare no competing financial interest.

ACKNOWLEDGMENT

We thank Professors Marc Hillmyer and Brooks Abel for invaluable discussion. This research was supported by the Center for Sustainable Polymers, a National Science Foundation (NSF) Center for Chemical Innovation (CHE-1901635) and Funds for International Cooperation and Exchange of the National Natural Science Foundation of China (Grant 21920102006). This study made use of the NMR Facility at Cornell University, which is supported, in part, by the NSF under Grant CHE-1531632. This work also made use of the Cornell Center for Materials Research shared instrumentation facility.

REFERENCES

(1) Paul, S.; Zhu, Y.; Romain, C.; Brooks, R.; Saini, P. K.; Williams, C. K. Ring-Opening Copolymerization (ROCOP): Synthesis and Properties of Polyesters and Polycarbonates. *Chem. Commun.* **2015**, *51*, 6459–6479.

(2) Lu, X.-B.; Ren, W.-M.; Wu, G.-P. CO_2 Copolymers from Epoxides: Catalyst Activity, Product Selectivity, and Stereochemistry Control. *Acc. Chem. Res.* **2012**, *45*, 1721–1735.

(3) Longo, J. M.; Sanford, M. J.; Coates, G. W. Ring-Opening Copolymerization of Epoxides and Cyclic Anhydrides with Discrete Metal Complexes: Structure–Property Relationships. *Chem. Rev.* **2016**, *116* , 15167–15197.

(4) Plajer, A. J.; Williams, C. K. Heterocycle/Heteroallene Ring-Opening Copolymerization: Selective Catalysis Delivering Alternating Copolymers. *Angew. Chem., Int. Ed.* **2022**, *61*, e202104495.

(5) Klaus, S.; Lehenmeier, M. W.; Anderson, C. E.; Rieger, B. Recent Advances in CO_2/Epoxide Copolymerization—New Strategies and Cooperative Mechanisms. *Coord. Chem. Rev.* **2011**, *255*, 1460–1479.

(6) Wang, Y.; Darensbourg, D. J. Carbon Dioxide-Based Functional Polycarbonates: Metal Catalyzed Copolymerization of CO_2 and Epoxides. *Coord. Chem. Rev.* **2018**, *372*, 85–100.

(7) Yang, G.-W.; Zhang, Y.-Y.; Wu, G.-P. Modular Organoboron Catalysts Enable Transformations with Unprecedented Reactivity. *Acc. Chem. Res.* **2021**, *54*, 4434–4448.

(8) Lidston, C. A. L.; Severson, S. M.; Abel, B. A.; Coates, G. W. Multifunctional Catalysts for Ring-Opening Copolymerizations. *ACS Catal.* **2022**, *12*, 11037–11070.

(9) Lu, X-B., Ren, B-H. Partners in Epoxide Copolymerization Catalysis: Approach to High Activity and Selectivity. *Chin. J. Polym. Sci.* **2022**, *40*, 1331–1348.

(10) Luo, M.; Zhang, X.-H.; Darensbourg, D. J. Poly(Monothiocarbonate)s from the Alternating and Regioselective Copolymerization of Carbonyl Sulfide with Epoxides. *Acc. Chem. Res.* **2016**, *49*, 2209–2219.

(11) Zhang, C.-J.; Zhang, X.-H. Recent Progress on COS-Derived Polymers. *Chin. J. Polym. Sci.* **2019**, *37*, 951–958.

(12) Yue, T.-J.; Ren, W.-M.; Lu, X.-B. Copolymerization Involving Sulfur-Containing Monomers. *Chem. Rev.* **2023**, *123*, 14038–14083.

(13) Uenishi, K.; Sudo, A.; Endo, T. Anionic Alternating Copolymerizability of Epoxide and 3,4-Dihydrocoumarin by Imidazole. *Macromolecules* **2007**, *40*, 6535–6539.

(14) Hosseini, K.; Goonesinghe, C.; Roshandel, H.; Chang, J.; Nyamayaro, K.; Jung, H.-J.; Diaconescu, P. L.; Mehrkhodavandi, P. Mechanistic Insights into Selective Indium-Catalyzed Coupling of Epoxides and Lactones. *ACS Catal.* **2023**, *13*, 13195–13204.

(15) Ren, F.; Liang, Z.-Z.; Niu, M.-X.; Hu, C.-Y.; Pang, X. Preparation of Chemically Recyclable Poly(Ether-Alt-Ester) by the Ring Opening Polymerization of Cyclic Monomers Synthesized by Coupling Glycolide and Epoxides. *Chin. J. Polym. Sci.* **2024**, *42*, 168–175.

(16) Jung, H.-J.; Goonesinghe, C.; Mehrkhodavandi, P. Temperature Triggered Alternating Copolymerization of Epoxides and Lactones *via* Pre-

Sequenced Spiroorthoester Intermediates. *Chem. Sci.* **2022**, *13*, 3713–3718.

(17) Sudo, A.; Zhang, Y.; Endo, T. Anionic Alternating Copolymerization of Epoxide and Six-membered Lactone Bearing Naphthyl Moiety. *J. Polym. Sci. A: Polym. Chem.* **2011**, *49*, 619–624.

(18) Chen, C.; Gnanou, Y.; Feng, X. Alternating Copolymerization of Epoxides with Isothiocyanates. *Macromolecules* **2021**, *54*, 9474–9481.

(19) Patil, N.; Gnanou, Y.; Feng, X. Anionic Copolymerization of *O*-Phthalaldehyde with Epoxides: Facile Access to Degradable Polyacetals and Their Copolymers under Ambient Conditions. *Macromolecules* **2022**, *55*, 7817–7826.

(20) Yu, X.; Hoffman, Z. J.; Lee, J.; Fang, C.; Gido, L. A.; Patel, V.; Eitouni, H. B.; Wang, R.; Balsara, N. P. A Practical Polymer Electrolyte for Lithium and Sodium Batteries: Poly(Pentyl Malonate). *ACS Energy Lett.* **2022**, *7*, 3791–3797.

(21) Fang, C.; Yu, X.; Chakraborty, S.; Balsara, N. P.; Wang, R. Molecular Origin of High Cation Transference in Mixtures of Poly(Pentyl Malonate) and Lithium Salt. *ACS Macro Lett.* **2023**, *12*, 612–618.

(22) Rowe, M. D.; Eyiler, E.; Walters, K. B. Hydrolytic Degradation of Bio-Based Polyesters: Effect of pH and Time. *Polym. Test.* **2016**, *52*, 192–199.

(23) Höglund, A.; Målberg, S.; Albertsson, A. Assessing the Degradation Profile of Functional Aliphatic Polyesters with Precise Control of the Degradation Products. *Macromol. Biosci.* **2012**, *12*, 260–268.

(24) Xie, X.; Zhang, P.; Li, X.; Wang, Z.; Qin, X.; Shao, M.; Zhang, L.; Zhou, W. Rational Design of F-Modified Polyester Electrolytes for Sustainable All-Solid-State Lithium Metal Batteries. *J. Am. Chem. Soc.* **2024**, *146*, 5940–5951.

(25) Byrne, F. P.; Assemat, J. M. Z.; Stanford, A. E.; Farmer, T. J.; Comerford, J. W.; Pellis, A. Enzyme-Catalyzed Synthesis of Malonate Polyesters and Their Use as Metal Chelating Materials. *Green Chem.* **2021**, *23*, 5043–5048.

(26) Kolb, N.; Meier, M. A. R. Monomers and Their Polymers Derived from Saturated Fatty Acid Methyl Esters and Dimethyl Carbonate. *Green Chem.* **2012**, *14*, 2429-2435.

(27) Lee, Y. Ionic Conductivity in the Poly(Ethylene Malonate)/Lithium Triflate System. *Solid State Ion.* **2001**, *138*, 273–276.

(28) Breton, P. Biocompatible Poly(Methylidene Malonate)-Made Materials for Pharmaceutical and Biomedical Applications. *Eur. J. Pharm. Biopharm.* **2008**, *68*, 479–495.

(29) Huang, M.; Liu, Y.; Yang, G.; Klier, J.; Schiffman, J. D. Anionic Polymerization of Methylene Malonate for High-Performance Coatings. *ACS Appl. Polym. Mater.* **2019**, *1*, 657–663.

(30) Higashimura, T.; Enoki, T.; Sawamoto, M. Living Cationic Polymerization of a Vinyl Ether with a Malonic Ester Function. *Polym. J.* **1987**, *19*, 515–521.

(31) Penelle, J.; Xie, T. Synthesis, Characterization, and Thermal Properties of Poly(Trimethylene-1,1-Dicarboxylate) Polyelectrolytes. *Macromolecules* **2001**, *34*, 5083–5089.

(32) Perrin, C. L. Malonic Anhydrides, Challenges from a Simple Structure. *J. Org. Chem.* **2022**, *87*, 7006–7012.

(33) Meldrum, A. N. A β-Lactonic Acid from Acetone and Malonic Acid. *J. Chem. Soc., Trans.* **1908**, *93*, 598–601.

(34) Davidson, D.; Bernhard, S. A.; The Structure of Meldrum's Supposed β-Lactonic Acid. *J. Am. Chem. Soc.* **1948**, *70*, 3426–3428.

(35) Leibfarth, F. A.; Hawker, C. J. The Emerging Utility of Ketenes in Polymer Chemistry. *J. Polym. Sci. Part A: Polym. Chem.* **2013**, *51*, 3769–3782.

(36) Lin, L.-K.; Wang, J.; Liu, Y.-L. Effective Synthesis Route for Linear and Cross-Linked Biodegradable Polyesters Using Aliphatic Meldrum's Acid Derivatives as Monomers. *ACS Omega* **2018**, *3*, 4641–4646.

(37) Chen, Y.-C.; Huang, C.-H.; Liu, Y.-L. Polymerization of Meldrum's Acid and Diisocyanate: An Effective Approach for Preparation of Reactive Polyamides and Polyurethanes. *ACS Omega* **2019**, *4*, 7884–7890.

(38) Meng, Q.; Gao, F.; Mosad, S.; Zhang, Z.; You, Y.; Hong, C. Facile Multicomponent Polymerization and Postpolymerization Modification via an Effective Meldrum's Acid-Based Three-Component Reaction. *Macromol. Rapid Commun.* **2021**, *42*, 2000610.

(39) Huang, C.-H.; Liu, Y.-L. Self-Polymerization of Meldrum's Acid-Amine Compounds: An Effective Route to Polyamides. *Polym. Chem.* **2021**, *12*, 291–298.

(40) Huang, C.-H.; Liu, Y.-L. The Michael Addition Reaction of Meldrum's Acid (MA): An Effective Route for the Preparation of Reactive Precursors for MA-Based Thermosetting Resins. *Polym. Chem.* **2019**, *10*, 1873–1881.

(41) Christensen, P. R.; Scheuermann, A. M.; Loeffler, K. E.; Helms, B. A. Closed-Loop Recycling of Plastics Enabled by Dynamic Covalent Diketoenamine Bonds. *Nat. Chem.* **2019**, *11*, 442–448.

(42) Trachsel, L.; Stewart, K. A.; Konar, D.; Hillman, J. D.; Moerschel, J. A.; Sumerlin, B. S. β-Triketones as Reactive Handles for Polymer Diversification via Dynamic Catalyst-Free Diketoenamine Click Chemistry. *J. Am. Chem. Soc.* **2024**, *146*, 16257–16267.

(43) Leibfarth, F. A.; Schneider, Y.; Lynd, N. A.; Schultz, A.; Moon, B.; Kramer, E. J.; Bazan, G. C.; Hawker, C. J. Ketene Functionalized Polyethylene: Control of Cross-Link Density and Material Properties. *J. Am. Chem. Soc.* **2010**, *132*, 14706–14709.

(44) Ishibashi, J. S. A.; Kalow, J. A. Vitrimeric Silicone Elastomers Enabled by Dynamic Meldrum's Acid-Derived Cross-Links. *ACS Macro Lett.* **2018**, *7*, 482–486.

(45) Yuan, L.; He, L.; Wang, Y.; Lang, X.; Yang, F.; Zhao, Y.; Zhao, H. Two- and Three-Component Post-Polymerization Modifications Based on Meldrum's Acid. *Macromolecules* **2020**, *53*, 3175–3181.

(46) Sun, X.; Chwatko, M.; Lee, D.-H.; Bachman, J. L.; Reuther, J. F.; Lynd, N. A.; Anslyn, E. V. Chemically Triggered Synthesis, Remodeling, and Degradation of Soft Materials. *J. Am. Chem. Soc.* **2020**, *142*, 3913–3922.

(47) Choi, G.; Oh, Y.; Jeong, S.; Chang, M.; Kim, H. Synthesis of Renewable, Recyclable, Degradable Thermosets Endowed with Highly Branched Polymeric Structures and Reinforced with Carbon Fibers. *Macromolecules* **2023**, *56*, 2526–2535.

(48) Lin, L.-K.; Hu, C.-C.; Su, W.-C.; Liu, Y.-L. Thermosetting Resins with High Fractions of Free Volume and Inherently Low Dielectric Constants. *Chem. Commun.* **2015**, *51*, 12760–12763.

(49) Huang, C.-H.; Liu, Y.-L. Self-Crosslinkable Polymers from Furan-Functionalized Meldrum's Acid and Maleimides as Effective Precursors of Free-Standing and Flexible Crosslinked Polymer Films Showing Low Dielectric Constants. *Polym. Chem.* **2020**, *11*, 1606–1613.

(50) González, L.; Ramis, X.; Salla, J. M.; Mantecón, A.; Serra, A. New Poly(Ether-ester) Thermosets Obtained by Cationic Curing of DGEBA and 7,7-dimethyl-6,8-dioxaspiro[3.5] Nonane-5,9-dione with Several Lewis Acids as Initiators. *J. Polym. Sci., Part A: Polym. Chem.* **2008**, *46*, 1229–1239.

(51) González, L.; Ramis, X.; Salla, J. M.; Serra, A.; Mantecón, A. New Thermosets Obtained from DGEBA and Meldrum Acid with Lanthanum and Ytterbium Triflates as Cationic Initiators. *Eur. Polym. J.* **2008**, *44*, 1535–1547.

(52) Wolffs, M.; Kade, M. J.; Hawker, C. J. An Energy Efficient and Facile Synthesis of High Molecular Weight Polyesters Using Ketenes. *Chem. Commun.* **2011**, *47*, 10572.

(53) Burke, D. J.; Kawauchi, T.; Kade, M. J.; Leibfarth, F. A.; McDearmon, B.; Wolffs, M.; Kierstead, P. H.; Moon, B.; Hawker, C. J. Ketene-Based Route to Rigid Cyclobutanediol Monomers for the Replacement of BPA in High Performance Polyesters. *ACS Macro Lett.* **2012**, *1*, 1228–1232.

(54) González, L.; Ramis, X.; Salla, J. M.; Mantecón, A.; Serra, A. Anionic Copolymerization of Diglycidyl Ether of Bisphenol A with Meldrum's Acid Derivatives Initiated by 4-(*N,N*-dimethylamino) Pyridine. *J. Appl. Polym. Sci.* **2009**, *111*, 1805–1815.

(55) Fieser, M. E.; Sanford, M. J.; Mitchell, L. A.; Dunbar, C. R.; Mandal, M.; Van Zee, N. J.; Urness, D. M.; Cramer, C. J.; Coates, G. W.; Tolman, W. B. Mechanistic Insights into the Alternating Copolymerization of Epoxides and Cyclic Anhydrides Using a (Salph)AlCl and Iminium Salt Catalytic System. *J. Am. Chem. Soc.* **2017**, *139*, 15222–15231.

(56) Thillaye Du Boullay, O.; Marchal, E.; Martin-Vaca, B.; Cossío, F. P.; Bourissou, D. An Activated Equivalent of Lactide toward Organocatalytic Ring-Opening Polymerization. *J. Am. Chem. Soc.* **2006**, *128*, 16442–16443.

(57) Martin Vaca, B.; Bourissou, D. *O*-Carboxyanhydrides: Useful Tools for the Preparation of Well-Defined Functionalized Polyesters. *ACS Macro Lett.* **2015**, *4*, 792–798.

(58) Neitzel, A. E.; Petersen, M. A.; Kokkoli, E.; Hillmyer, M. A. Divergent Mechanistic Avenues to an Aliphatic Polyesteracetal or Polyester from a Single Cyclic Esteracetal. *ACS Macro Lett.* **2014**, *3*, 1156–1160.

(59) Cairns, S. A.; Schultheiss, A.; Shaver, M. P. A Broad Scope of Aliphatic Polyesters Prepared by Elimination of Small Molecules from Sustainable 1,3-Dioxolan-4-Ones. *Polym. Chem.* **2017**, *8*, 2990–2996.

(60) Xu, Y.; Şucu, T.; Perry, M. R.; Shaver, M. P. Alicyclic Polyesters from a Bicyclic 1,3-Dioxane-4-One. *Polym. Chem.* **2020**, *11*, 4928–4932.

(61) Xu, Y.; Perry, M. R.; Cairns, S. A.; Shaver, M. P. Understanding the Ring-Opening Polymerisation of Dioxolanones. *Polym. Chem.* **2019**, *10*, 3048–3054.

(62) Şucu, T.; Wang, M.; Shaver, M. P. Degradable and Reprocessable Resins from a Dioxolanone Cross-Linker. *Macromolecules* **2023**, *56*, 1625–1632.

(63) Billington, E. K.; Şucu, T.; Shaver, M. P. Mechanical Properties and Recyclability of Fiber Reinforced Polyester Composites. *ACS Sustainable Chem. Eng.* **2024**, *12*, 10011–10019.

(64) Byun, K.; Mo, Y.; Gao, J. New Insight on the Origin of the Unusual Acidity of Meldrum's Acid from Ab Initio and Combined QM/MM Simulation Study. *J. Am. Chem. Soc.* **2001**, *123*, 3974–3979.

(65) Abel, B. A.; Lidston, C. A. L.; Coates, G. W. Mechanism-Inspired Design of Bifunctional Catalysts for the Alternating Ring-Opening Copolymerization of Epoxides and Cyclic Anhydrides. *J. Am. Chem. Soc.* **2019**, *141*, 12760–12769.

(66) Tsai, F.-T.; Wang, Y.; Darensbourg, D. J. Environmentally Benign CO_2 -Based Copolymers: Degradable Polycarbonates Derived from Dihydroxybutyric Acid and Their Platinum–Polymer Conjugates. *J. Am. Chem. Soc.* **2016**, *138*, 4626–4633.

(67) Lidston, C. A. L.; Abel, B. A.; Coates, G. W. Bifunctional Catalysis Prevents Inhibition in Reversible-Deactivation Ring-Opening Copolymerizations of Epoxides and Cyclic Anhydrides. *J. Am. Chem. Soc.* **2020**, *142*, 20161–20169.

(68) Darensbourg, D. J. Chain Transfer Agents Utilized in Epoxide and CO_2 Copolymerization Processes. *Green Chem.* **2019**, *21*, 2214–2223.

(69) Nejad, E. H.; van Melis, C. G. W.; Vermeer, T. J.; Koning, C.E.; Duchateau, R. Alternating Ring-Opening Polymerization of Cyclohexene Oxide and Anhydrides: Effect of Catalyst, Cocatalyst, and Anhydride Structure. *Macromolecules* **2012**, *45*, 1770–1776.

(70) Darensbourg, D. J.; Yeung, A. D. A Concise Review of Computational Studies of the Carbon Dioxide–Epoxide Copolymerization Reactions. *Polym. Chem.* **2014**, *5*, 3949–3962.

(71) Allen, A. D.; Tidwell, T. T. New Directions in Ketene Chemistry: The Land of Opportunity. *Eur. J. Org. Chem.* **2012**, 1081–1096.

(72) Pair, E.; Cadart, T.; Levacher, V.; Brière, J. Meldrum's Acid: A Useful Platform in Asymmetric Organocatalysis. *ChemCatChem.* **2016**, *8*, 1882–1890.

(73) Wang, S.-X.; Wang, M.-X.; Wang, D.-X.; Zhu, J. Chiral Salen–Aluminum Complex as a Catalyst for Enantioselective α-Addition of Isocyanides to Aldehydes: Asymmetric Synthesis of 2-(1-Hydroxyalkyl)-5-Aminooxazoles. *Org. Lett.* **2007**, *9*, 3615–3618.

(74) Zhou, D.; Shanmukaraj, D.; Tkacheva, A.; Armand, M.; Wang, G. Polymer Electrolytes for Lithium-Based Batteries: Advances and Prospects. *Chem.* **2019**, *5*, 2326–2352.

(75) Zhou, Z.; LaPointe, A. M.; Coates, G. W. Atactic, Isotactic, and Syndiotactic Methylated Polyhydroxybutyrates: An Unexpected Series of Isomorphic Polymers. *J. Am. Chem. Soc.* **2023**, *145*, 25983-25988.

(76) Scoti, M.; Zhou, L.; Chen, E. Y.-X.; De Rosa, C. Crystal Structure of Atactic and Isotactic Poly(3-Hydroxy-2,2-Dimethylbutyrate): A Chemically Recyclable Poly(Hydroxyalkanoate) with Tacticity-Independent Crystallinity. *Macromolecules* **2024**, *57*, 4357–4373.

TOC Graphic

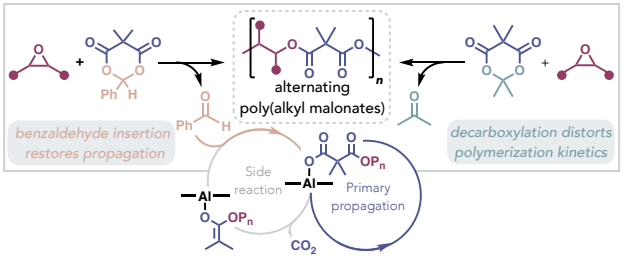
alternating
poly(alkyl malonates)
benzaldehyde insertion
restores propagation
decarboxylation distorts
polymerization kinetics
Side
reaction
Primary
propagation
Al
OPn
CO2